

# Cosmographic analysis with Chebyshev polynomials

Salvatore Capozziello,<sup>1,2,3,\*</sup> Rocco D’Agostino,<sup>4,5,†</sup> and Orlando Luongo<sup>6,7,8,9,‡</sup>

<sup>1</sup>*Dipartimento di Fisica, Università di Napoli “Federico II”, Via Cinthia, I-80126, Napoli, Italy.*

<sup>2</sup>*Istituto Nazionale di Fisica Nucleare (INFN), Sez. di Napoli, Via Cinthia 9, I-80126 Napoli, Italy.*

<sup>3</sup>*Gran Sasso Science Institute, Via F. Crispi 7, I-67100, L’Aquila, Italy.*

<sup>4</sup>*Dipartimento di Fisica, Università degli Studi di Roma “Tor Vergata”,  
Via della Ricerca Scientifica 1, I-00133, Roma, Italy.*

<sup>5</sup>*Istituto Nazionale di Fisica Nucleare (INFN), Sez. di Roma “Tor Vergata”,  
Via della Ricerca Scientifica 1, I-00133, Roma, Italy.*

<sup>6</sup>*Istituto Nazionale di Fisica Nucleare, Laboratori Nazionali di Frascati, 00044 Frascati, Italy.*

<sup>7</sup>*School of Science and Technology, University of Camerino, I-62032, Camerino, Italy.*

<sup>8</sup>*Department of Mathematics and Applied Mathematics,  
University of Cape Town, Rondebosch 7701, Cape Town, South Africa.*

<sup>9</sup>*Astrophysics, Cosmology and Gravity Centre (ACGC),  
University of Cape Town, Rondebosch 7701, Cape Town, South Africa.*

The limits of standard cosmography are here revised addressing the problem of error propagation during statistical analyses. To do so, we propose the use of Chebyshev polynomials to parameterize cosmic distances. In particular, we demonstrate that building up rational Chebyshev polynomials significantly reduces error propagations with respect to standard Taylor series. This technique provides unbiased estimations of the cosmographic parameters and performs significantly better than previous numerical approximations. To figure this out, we compare rational Chebyshev polynomials with Padé series. In addition, we theoretically evaluate the convergence radius of (1,1) Chebyshev rational polynomial and we compare it with the convergence radii of Taylor and Padé approximations. We thus focus on regions in which convergence of Chebyshev rational functions is better than standard approaches. With this recipe, as high-redshift data are employed, rational Chebyshev polynomials remain highly stable and enable one to derive highly accurate analytical approximations of Hubble’s rate in terms of the cosmographic series. Finally, we check our theoretical predictions by setting bounds on cosmographic parameters through Monte Carlo integration techniques, based on the Metropolis-Hastings algorithm. We apply our technique to high-redshift cosmic data, using the JLA supernovae sample and the most recent versions of Hubble parameter and baryon acoustic oscillation measurements. We find that cosmography with Taylor series fails to be predictive with the aforementioned data sets, while turns out to be much more stable using the Chebyshev approach.

## I. INTRODUCTION

The cosmic acceleration is today confirmed by a large number of observations [1, 2] and represents a consolidate challenge of modern cosmology. To disclose the physics behind it, model-independent techniques have been widely investigated during last years. Strategies toward model-independent treatments have as main target the determination of universe’s expansion history without the need of postulating *a priori* dark energy contributions. A particular attention is currently given to *cosmography* [4–12]. Standard cosmography lies on Taylor expansions of cosmic distances. The method provides a powerful tool to study the dark energy evolution without assuming its functional form in the Hubble rate. Moreover, fixing limits over free cosmographic parameters alleviates degeneracy among models and enables to understand which paradigms are effectively favored directly with respect to data surveys. Although cosmography

candidates as a robust tool to understand whether dark energy evolves or not, cosmic data unfortunately span on intervals  $z \geq 1$ . This limit poses severe restrictions on cosmography and makes inapplicable Taylor expansions built up around  $z \simeq 0$ .

One stratagem to overcome this problem is to parameterize Taylor expansions in terms of *auxiliary variables*. Unfortunately, even this case turns out to be jeopardized by severe error propagations over the final outcomes. More recently, a further effort has been the use of Padé approximation built up to converge at higher redshift domains [13, 14]. In this case, however, the expansion orders are not fixed *a priori* and this causes difficulties on evaluating the rate of convergence as  $z \rightarrow \infty$ . Thus, the limits of standard Taylor approach lying on  $z \geq 1$  are essentially alleviated but not fully fixed.

Motivated by the need of reducing relative uncertainties in cosmography, we here propose a new cosmographic technique based on Chebyshev polynomials. Chebyshev polynomials represent sequences of orthogonal polynomials, recursively-defined through trigonometric functions. In our approach we develop a new *Chebyshev cosmography* adopting the strategy of building up rational approximations made by these polynomial functions.

---

\* capozzie@na.infn.it

† rocco.dagostino@roma2.infn.it

‡ orlando.luongo@lnf.infn.it

We demonstrate that, under the hypothesis of rational Chebyshev polynomials, distinguishing Chebyshev functions of first and second kinds is not relevant since the final output gives analogous results in both the cases. For simplicity, we limit our analysis on first kind Chebyshev polynomials only and we write the sequence of Chebyshev rational functions which better approximate Taylor series up to a certain order. We thus show that our Chebyshev ratios provide nodes in polynomial interpolation, minimizing cosmographic uncertainties leading to the most likely well-motivated approximation to cosmic distances. We even present theoretical motivations behind our choice by computing the convergence radii for different choices of polynomial approximations.

To check how well our model works we also study Padé expansions and we compare the Chebyshev technique with them. We finally show the advantages of our procedure with respect to the old approaches using data surveys, confronting the cosmological quantities built from our method with the observables of the latest cosmological data sets. We adopt a Monte Carlo analysis employing the Metropolis-Hastings algorithm, choosing JLA supernova, baryon acoustic oscillation and differential age measurements. We show the goodness of our procedures comparing the outcomes coming from standard cosmography and our method, showing that error uncertainties are effectively reduced.

The structure of the paper is as follows. In Sec. II, we review the general aspects of cosmography. In Sec. III, we describe the mathematical features of the Chebyshev polynomials and present the method of the rational Chebyshev approximations. In Sec. IV, we derive a new model-independent formula for the luminosity distance, and compare the new method with the standard cosmographic procedures to verify the goodness of our approach. In Sec. V, we place observational limits on the cosmographic parameters through a confront with the most recent experimental data. Finally, in Sec. VI we summarize our findings and conclude.

## II. THE COSMOGRAPHIC APPROACH

The study of the cosmic evolution can be done independently of energy densities by means of cosmography. This model-independent technique only relies on the observationally justifiable assumptions of homogeneity and isotropy [15–17]. The great advantage of this method is that it allows one to reconstruct the dynamical evolution of the dark energy term without assuming any particular cosmological model. Cosmography involves Taylor expansions of observable quantities that may, in principle, go up to any order. These expansions can be compared directly with data. The outcomes of this procedure ensure the independence from any postulated equation of state governing the evolution of the universe and, thus, help to break the degeneracy among cosmological models.

The homogenous and isotropic universe is governed by the single degree of freedom offered by  $a(t)$ , as demanded by the cosmological principle. Hence, following the most recent measurements of [3] and assuming a spatially flat universe<sup>1</sup>, we can expand  $a(t)$  in Taylor series around present time  $t_0$  [19, 20]:

$$a(t) = 1 + \sum_{k=1}^{\infty} \frac{1}{k!} \frac{d^k a}{dt^k} \Big|_{t=t_0} (t - t_0)^k, \quad (1)$$

where  $a(t_0) = 1$ .

The expansion above defines the cosmographic series [21–25]:

$$H \equiv \frac{1}{a} \frac{da}{dt}, \quad q \equiv -\frac{1}{aH^2} \frac{d^2 a}{dt^2}, \quad (2)$$

$$j \equiv \frac{1}{aH^3} \frac{d^3 a}{dt^3}, \quad s \equiv \frac{1}{aH^4} \frac{d^4 a}{dt^4}, \quad (3)$$

known in the literature as *Hubble*, *deceleration*, *jerk* and *snap* parameters<sup>2</sup>. These coefficients are used to describe the expansion history of the universe at late times.

Using the relation  $z = a^{-1} - 1$  and Eq. (1), one finds the Taylor series expansion of the luminosity distance as function of the redshift [26–29]:

$$d_L(z) = \frac{c}{H_0} z \left[ 1 + \frac{z}{2}(1 - q_0) - \frac{z^2}{6}(1 - q_0 - 3q_0^2 + j_0) + \frac{z^3}{24}(2 - 2q_0 - 15q_0^2 - 15q_0^3 + 5j_0 + 10q_0j_0 + s_0) + \mathcal{O}(z^4) \right]. \quad (4)$$

The above expression for the luminosity distance can be used to obtain limits on the cosmographic parameters and study the low- $z$  dynamics of the universe with no need of any *a priori* assumed cosmological model. In fact, plugging Eq. (4) into the definition

$$H(z) = c \left[ \frac{d}{dz} \left( \frac{d_L(z)}{(1+z)} \right) \right]^{-1}, \quad (5)$$

one gets

$$H(z) \simeq H_0 \left[ 1 + H^{(1)}z + H^{(2)}\frac{z^2}{2} + H^{(3)}\frac{z^3}{6} \right], \quad (6a)$$

$$H^{(1)} = 1 + q_0, \quad (6b)$$

$$H^{(2)} = j_0 - q_0^2, \quad (6c)$$

$$H^{(3)} = 3q_0^2 + 3q_0^3 - j_0(3 + 4q_0) - s_0, \quad (6d)$$

which describes the expansion history of the late-time universe up to the snap parameter.

<sup>1</sup> The assumption of flatness overcomes problems of degeneracy among the cosmographic parameters entering the expression of the luminosity distance [18].

<sup>2</sup> In principle, one may go further in the expansion and consider higher order coefficients. We limit our study up to the *snap*, since the next cosmographic parameters are poorly constrained by observations [25].

### A. The convergence problem

The limits of the standard cosmographic approach, based on the Taylor approximations, emerge when cosmological data at high redshifts are used to get information on the evolution of the dark energy term. In fact, the Taylor series converges if  $z < 1$ , so that any cosmographic analysis employing data beyond this limit is plagued by severe restrictions. A way to extend the radius of convergence of the Taylor series to high-redshift domains is represented by the method of rational approximations, among which the Padé polynomials represent a relevant example [30]. The Taylor expansion of a generic function  $f(z)$  is  $f(z) = \sum_{i=0}^{\infty} c_i z^i$ , where  $c_i = f^{(i)}(0)/i!$ , whereas one defines the  $(n, m)$  Padé approximant of  $f(z)$  as the rational polynomial

$$P_{n,m}(z) = \frac{\sum_{i=0}^n a_i z^i}{1 + \sum_{j=1}^m b_j z^j}. \quad (7)$$

Since by construction one requires that  $b_0 = 1$ , we have:

$$f(z) - P_{n,m}(z) = \mathcal{O}(z^{n+m+1}). \quad (8)$$

The coefficients  $b_i$  in Eq. (7) are thus determined by solving the following homogeneous system of linear equations [31]:

$$\sum_{j=1}^m b_j c_{n+k+j} = -b_0 c_{n+k}, \quad (9)$$

valid for  $k = 1, \dots, m$ . All coefficients  $a_i$  in Eq. (7) may be computed using the formula

$$a_i = \sum_{k=0}^i b_{i-k} c_k. \quad (10)$$

The technique of Padé approximations has been recently investigated in the context of cosmography to handle the divergence problems at high- $z$  domains [13, 14]. In the next section, we present the method of rational Chebyshev polynomials that we will use to obtain a new cosmographic expression for the luminosity distance.

### III. RATIONAL CHEBYSHEV POLYNOMIALS

The method we propose here aims to optimize the technique of rational polynomials and consists of approximating the luminosity distance with a ratio of Chebyshev polynomials. In fact, the Padé approximants are built up from the Taylor approximation of  $d_L(z)$  whose error bars, by construction, rapidly increase as the redshift departs from zero. Motivated by this issue, we exploit the Chebyshev polynomials. Such a choice aims at reducing

the uncertainties on the estimate of the cosmographic parameters.

The Chebyshev polynomials<sup>3</sup>  $T_n(z)$  are defined through the identity

$$T_n(z) = \cos(n\theta), \quad (11)$$

where  $\theta = \arccos(z)$  and  $n \in \mathbb{N}_0$ . They form an orthogonal set with respect to the weighting function  $w(z) = (1 - z^2)^{-1/2}$  in the domain  $|z| \leq 1$  [32]:

$$\int_{-1}^1 T_n(z) T_m(z) w(z) dz = \begin{cases} \pi, & n = m = 0 \\ \frac{\pi}{2} \delta_{nm}, & \text{otherwise} \end{cases} \quad (12)$$

where  $\delta_{nm}$  is the Kronecker delta. The Chebyshev polynomials are generated from the recurrence relation

$$T_{n+1}(z) = 2zT_n(z) - T_{n-1}(z). \quad (13)$$

The explicit expressions of the first five polynomials<sup>4</sup> that we will employ to build the new expression for  $d_L(z)$  read [33]:

$$\begin{aligned} T_0(z) &= 1, \\ T_1(z) &= z, \\ T_2(z) &= 2z^2 - 1, \\ T_3(z) &= 4z^3 - 3z, \\ T_4(z) &= 8z^4 - 8z^2 + 1. \end{aligned} \quad (14)$$

It is possible to express the powers of  $z$  in terms of the Chebyshev polynomials according to the formula [31]:

$$z^n = 2^{1-n} \sum_{k=0}^{[n/2]} a_k \binom{n}{k} T_{n-2k}(z), \quad (15)$$

for  $n > 0$ . Here,  $[n/2]$  is the integer part of  $n/2$ ,  $a_k = 1/2$  if  $k = n/2$  and  $a_k = 1$  if  $a_k \neq n/2$ , and  $\binom{n}{k}$  are the binomial coefficients.

Let  $f(z) \in L_w^2$ , being  $L_w^2$  the Hilbert space of the square-integrable functions with respect to the measure  $w^{-1}(z) dz$ . Suppose we know the truncated Taylor series of  $f(z)$  around the point  $z = 0$ ,  $g(z)$ . It is possible to obtain the polynomial of degree  $n$ ,  $\sum_{k=0}^n c_k T_k$ , which gives the best approximation of  $f(z)$  in the interval  $[-1, 1]$  in  $L_w^2$ . Formally, the Chebyshev series expansion of  $f(z)$  reads

$$f(z) = \sum_{k=0}^{\infty} c_k T_k(z), \quad (16)$$

<sup>3</sup> Throughout the text, we refer to the Chebyshev polynomials of the *first kind* simply as Chebyshev polynomials.

<sup>4</sup> We here truncate our analysis to the fifth order, since additional contributions go beyond our treatment. In so doing, we arrive to analyse up to snap parameter  $s_0$ .

where

$$\begin{cases} c_0 = \frac{1}{\pi} \int_{-1}^1 g(z) T(z) w(z) dz , \\ c_k = \frac{2}{\pi} \int_{-1}^1 g(z) T(z) w(z) dz , \quad k > 0 . \end{cases} \quad (17)$$

Hence, we define the  $(n, m)$  rational Chebyshev approximant as

$$R_{n,m}(z) = \frac{\sum_{i=0}^n a_i T_i(z)}{\sum_{j=0}^m b_j T_j(z)} . \quad (18)$$

For  $b_0 \neq 0$ , through a redefinition of the coefficients, we can recast Eq. (18) in the form

$$R_{n,m}(z) = \frac{\sum_{i=0}^n a_i T_i(z)}{1 + \sum_{j=1}^m b_j T_j(z)} . \quad (19)$$

Applying a similar procedure used to obtain the Padé approximants, one can calculate the unknown coefficients  $a_k$  and  $b_k$  by equating Eq. (16) and Eq. (19) up to the  $(n+m)$ -th Chebyshev polynomial:

$$\sum_{k=0}^{\infty} c_k T_k = \frac{\sum_{i=0}^n a_i T_i}{1 + \sum_{j=1}^m b_j T_j} + \mathcal{O}(T_{n+m+1}) . \quad (20)$$

By doing so, one gets:

$$(1 + b_1 T_1 + \dots + b_m T_m)(c_0 + c_1 T_1 + \dots) = a_0 + a_1 T_1 + \dots + a_n T_n + \mathcal{O}(T_{n+m+1}) . \quad (21)$$

To calculate the products of Chebyshev polynomials that occur in the left hand side of Eq. (21), one can make use of the trigonometric identity

$$\cos(n\theta) \cos(m\theta) = \frac{1}{2} [\cos[(n+m)\theta] + \cos[(n-m)\theta]] ,$$

which leads to the relation

$$T_n(z) T_m(z) = \frac{1}{2} [T_{n+m}(z) + T_{|n-m|}(z)] . \quad (22)$$

Thus, equating the terms with the same degree of  $T$ 's yields  $(n+m+1)$  equations for the  $(n+m+1)$  unknowns in Eq. (19).

In the next section, we apply the mathematical procedure we have presented above to find a very accurate model-independent expression for the luminosity distance. We also compare our method with the cosmographic approaches developed so far in the literature.

#### IV. THE CHEBYSHEV COSMOGRAPHY

We are here interested in approximating the luminosity distance with rational Chebyshev polynomials. First, we need to express  $d_L(z)$  in terms of Chebyshev polynomials according to Eq. (16). To do that, we calculate the coefficients  $c_k$  in Eq. (17) where, in our case,  $g(z)$  is the Taylor expansion given in Eq. (4). Hence, the fourth-order Chebyshev expansion of the luminosity distance can be expressed as

$$d_L(z) = \frac{c}{H_0} \sum_{n=0}^4 c_n T_n(z) , \quad (23)$$

where the coefficients  $c_n$  read:

$$\begin{aligned} c_0 &= \frac{1}{64} [18 + 5j_0(1 + 2q_0) - 3q_0(6 + 5q_0(1 + q_0)) + s_0] , \\ c_1 &= \frac{1}{8} (7 - j_0 + q_0 + 3q_0^2) , \\ c_2 &= \frac{1}{48} [14 + 5j_0(1 + 2q_0) - q_0(14 + 15q_0(1 + q_0)) + s_0] , \\ c_3 &= \frac{1}{24} (-1 - j_0 + q_0(1 + 3q_0)) , \\ c_4 &= \frac{1}{192} [2 + 5j_0(1 + 2q_0) - q_0(2 + 15q_0(1 + q_0)) + s_0] . \end{aligned}$$

Thus, one can construct the rational Chebyshev approximations of  $d_L(z)$  as in Eq. (19) starting from Eq. (23). We report some explicit expressions in Appendix A. Polynomials of high degrees will lead to more accurate approximations, even though these are the ones characterized by more complicated analytical forms, of course.

##### A. Calibrating Chebyshev polynomials with the concordance model

To check the accuracy of various Chebyshev approximations, we compare them with the  $\Lambda$ CDM luminosity distance,  $d_L(z)|_{\Lambda\text{CDM}}$ :

$$d_L(z)|_{\Lambda\text{CDM}} = (1+z) \int_0^z \frac{c dz'}{H_{\Lambda\text{CDM}}(z')} , \quad (24)$$

in which we have:

$$H_{\Lambda\text{CDM}}(z) = H_0 \sqrt{\Omega_{m0}(1+z)^3 + \Omega_{\Lambda}} . \quad (25)$$

According to a spatially flat universe, we set  $\Omega_{\Lambda} = 1 - \Omega_{m0}$ , having  $\Omega_{m0}$  the matter density at current time. In the concordance paradigm case, the cosmographic parameters can be calculated in terms of  $\Omega_{m0}$ :

$$\begin{aligned} q_{0,\Lambda\text{CDM}} &= -1 + \frac{3}{2} \Omega_{m0} , \\ j_{0,\Lambda\text{CDM}} &= 1 , \\ s_{0,\Lambda\text{CDM}} &= 1 - \frac{9}{2} \Omega_{m0} . \end{aligned} \quad (26)$$

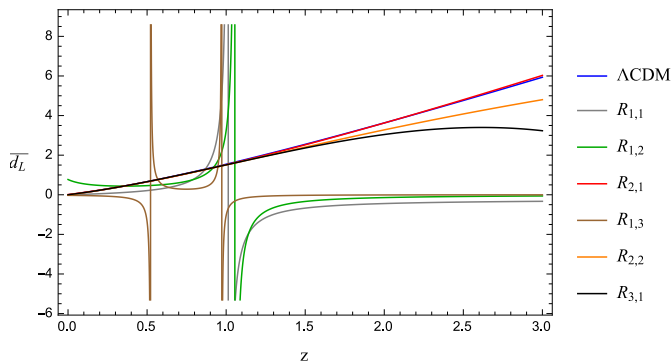


FIG. 1. Dimensionless luminosity distance as function of the redshift for rational Chebyshev approximations of the second ( $R_{1,1}$ ), third ( $R_{1,2}$ ,  $R_{2,1}$ ) and fourth ( $R_{1,3}$ ,  $R_{2,2}$ ,  $R_{3,1}$ ) degrees, compared to the  $\Lambda$ CDM model.

As an indicative possibility, we fix  $\Omega_{m0} = 0.3$ . So that from Eq. (26) one gets:

$$\begin{cases} q_0 = -0.55, \\ j_0 = 1, \\ s_0 = -0.35. \end{cases} \quad (27)$$

Using the values of Eq. (27), in Fig. 1 we show the behaviour with the redshift of  $\bar{d}_L(z) \equiv \frac{H_0}{c} d_L(z)$  for different degrees of rational Chebyshev approximations. In principle, to approximate the  $\Lambda$ CDM model some of the rational Chebyshev polynomials may present singularities turning out to give unsuitable outcomes. To overcome this issue, the preferred rational approximations are those with  $n - m \geq 0$ , in analogy to what happens for Padé approximations [34]. In particular, as practically checked the approximant  $R_{2,1}(z)$  seems to give the most accurate approximation to the luminosity distance of the  $\Lambda$ CDM model. Assuming that the calibration with the concordance paradigm would be viable for any possible dark energy term, we assume that the most suitable approximation with Chebyshev polynomials comes from  $R_{2,1}(z)$ .

To portray a qualitative representation of numerical improvements that one gains using our method, we compare  $R_{2,1}(z)$  with the standard fourth-order Taylor expansion of  $d_L(z)$  given in Eq. (4), and with the (2,2) Padé approximation of  $d_L(z)$ . We choose the (2,2) Padé approximation since it has been argued that it is robustly characterized by good convergence properties [34] as used in computational analyses. We note that, while in the Taylor and Padé approximations the *snap* parameter shows up at the fourth order, in the rational Chebyshev polynomials it is present from the lowest degrees, since all the coefficients  $c_k$  of Eq. (23) have been calculated from the Taylor series expansion of  $d_L(z)$  up to the *snap* order (as confirmed in Eq. (4)). For comparison, we report the expression of the (2,2) Padé approximation of  $d_L(z)$  in Appendix B. In Fig. 2, we show the behaviour of  $\bar{d}_L(z)$

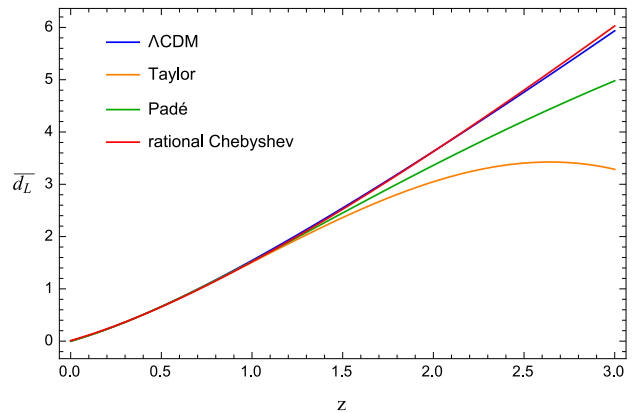


FIG. 2. Dimensionless luminosity distance as function of the redshift for the  $\Lambda$ CDM model and its fourth-order Taylor, (2,2) Padé and (2,1) rational Chebyshev approximations.

for the various techniques. As can be seen, the Taylor approach fails when  $z > 1$ . Our Chebyshev cosmography stands out for the excellent approximation to the  $\Lambda$ CDM luminosity distance, resulting mostly more effective than Padé approximations.

## B. The convergence radius

We here argue how to *broadcast* the above considerations to well-motivated theoretical scenarios. Thus, we wonder whether Chebyshev cosmography is expected to effectively improve the approximations to cosmic distances than standard cosmography. To do so, it behooves us to check how much the aforementioned approximations are stable to higher redshifts. Hence, one can test the ability of the various cosmographic techniques, able to describe high-redshift domains, by a direct comparison among the corresponding convergence radii, here defined by  $\rho$ .

As a simple example, we explicitly calculate the convergence radius of the (1,1) rational Chebyshev approximation of the luminosity distance, compared to the second-order Taylor series and to the (1,1) Padé approximation. From Eqs. (14) and (19), it holds

$$R_{1,1}(z) = \frac{a_0 T_0(z) + a_1 T_1(z)}{1 + b_1 T_1(z)} = \frac{a_0 + a_1 z}{1 + b_1 z}, \quad (28)$$

where the coefficients  $\{a_0, a_1, b_1\}$  are expressed in terms of the cosmographic series as shown in Eq. (A1). We can rearrange Eq. (28) as

$$R_{1,1} = \frac{a_0}{1 + b_1 z} + \frac{a_1}{b_1} \left( 1 - \frac{1}{1 + b_1 z} \right), \quad (29)$$

and, after some algebra, one obtains

$$R_{1,1} = \frac{a_1}{b_1} + \left( a_0 - \frac{a_1}{b_1} \right) \sum_{n=0}^{\infty} (-b_1)^n z^n. \quad (30)$$

The geometric series in Eq. (30) converges for  $|z| < 1/|b_1|$ , so that the convergence radius of the (1,1) rational Chebyshev approximation of  $d_L(z)$  is

$$\begin{aligned} \rho_{R_{1,1}} &= \frac{1}{|b_1|} \\ &= \left| \frac{-3(7 - j_0 + q_0 + 3q_0^2)}{14 + 5j_0(1 + 2q_0) - q_0(14 + 15q_0(1 + q_0)) + s_0} \right|. \end{aligned} \quad (31)$$

Analogous calculations show that the convergence radius of the (1,1) Padé approximant for  $d_L(z)$  is

$$\rho_{P_{1,1}} = \frac{2}{1 - q_0}. \quad (32)$$

The convergence radius of the second-order Taylor series of  $d_L(z)$  is approximately given by

$$\rho_{d_{L,2}} = \frac{1 - q_0}{2}. \quad (33)$$

For the sake of completeness, the numerical values of  $\rho_{R_{1,1}}$ ,  $\rho_{P_{1,1}}$  and  $\rho_{d_{L,2}}$  should be computed by using fitting results over the cosmographic coefficients. However, an analogous check can be made assuming the reference values Eq. (26). In such a case, one gets:

$$\begin{cases} \rho_{R_{1,1}} = 1.014, \\ \rho_{P_{1,1}} = 1.290, \\ \rho_{d_{L,2}} = 0.775. \end{cases} \quad (34)$$

These indicative results confirm the improvements of the rational polynomials in extending the radius of convergence with respect to the Taylor series. From the outcomes of Eq. (26) we notice that the convergence radius of the Padé approximation seems fairly better than the Chebyshev one. However, this is due to the choice made on the set  $q_0$ ,  $j_0$  and  $s_0$ . In Fig. 3 we plot the convergence radii for Taylor, Padé and Chebyshev polynomials with a different set of cosmographic coefficients not calibrated over the concordance paradigm. In Fig. 3, in particular, we show the regions in which the improvements of Chebyshev rational approximations become significant in terms of the convergence radius.

## V. OBSERVATIONAL CONSTRAINTS

In this section, we present the data we use to set bounds on the cosmographic parameters.

### A. Supernovae Ia

In the present work, we test the Joint Light-curve Analysis (JLA) sample of 740 SNe of type Ia [35] in the redshift interval  $0.01 < z < 1.3$ . All the SNe have been

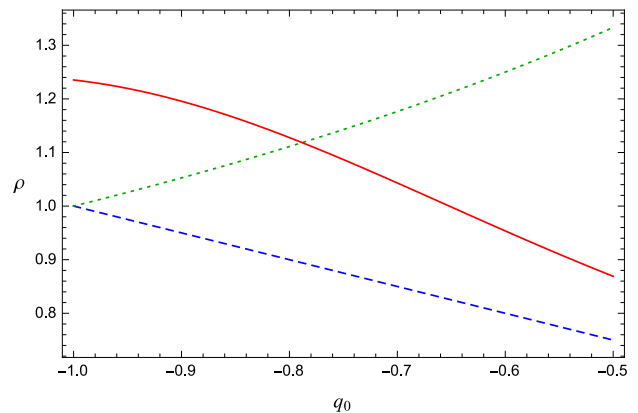


FIG. 3. Convergence radii for the second-order Taylor (dashed curve), (1,1) Padé (dotted curve) and (1,1) rational Chebyshev (solid curve) approximations of the luminosity distance as a function of  $q_0$ . For the rational Chebyshev approximation we used the indicative values of  $j_0 = 2$ ,  $s_0 = -1$ .

standardized using the SALT2 model [36] as fitter for their light curves. The catalogue provides, for each SN, the redshift  $z$ , model-independent apparent magnitude in the  $B$  band ( $m_B$ ), the stretch factor of the light-curve ( $X_1$ ), and the colour at maximum brightness ( $C$ ). The theoretical distance modulus,

$$\mu_{th}(z) = 25 + 5 \log_{10}[d_L(z)], \quad (35)$$

is parametrized as follows:

$$\mu_{obs} = m_B - (M_B - \alpha X_1 + \beta C), \quad (36)$$

where the absolute magnitude is defined as

$$M_B = \begin{cases} M, & \text{if } M_{host} < 10^{10} M_{Sun} \\ M + \Delta_M, & \text{otherwise} \end{cases} \quad (37)$$

being  $M_{host}$  the host stellar mass. The nuisance parameters  $\{M, \Delta_M, \alpha, \beta\}$  are fitted together with the cosmological parameters. The normalized likelihood function of the SNe data is given by

$$\mathcal{L}_{SN} = \frac{1}{|2\pi\mathbf{C}|^{1/2}} \exp \left[ -\frac{1}{2} (\mu_{th} - \mu_{obs})^\dagger \mathbf{C}^{-1} (\mu_{th} - \mu_{obs}) \right], \quad (38)$$

where  $\mathbf{C}$  is the  $2220 \times 2200$  covariance matrix constructed as in [35], which includes statistical and systematic uncertainties on the light-curve parameters.

### B. Observational Hubble Data

The Hubble rate of a given cosmological model can be constrained by means of the model-independent measurements acquired through the differential age (DA) method, first presented in [37]. Such a technique uses

red passively evolving galaxies as cosmic chronometers. In particular, one can obtain  $H(z)$  by measuring the age difference of two close galaxies and using the relation:

$$H_{th}(z) = -\frac{1}{(1+z)} \left( \frac{dt}{dz} \right)^{-1}. \quad (39)$$

The normalized likelihood function for the OHD data ( $\mathcal{L}_{OHD}$ ) is built using a collection of 31 uncorrelated DA measurements of  $H(z)$ , which we report in Appendix C:

$$\mathcal{L}_{OHD} = \frac{\exp \left[ -\frac{1}{2} \sum_{i=1}^{31} \left( \frac{H_{th}(z_i) - H_{obs}(z_i)}{\sigma_{H,i}} \right)^2 \right]}{\left[ (2\pi)^{31} \prod_{i=1}^{31} \sigma_{H,i}^2 \right]^{1/2}}. \quad (40)$$

### C. Baryon Acoustic Oscillations

Intensive studies on the large scale structures of the universe have been done thanks to galaxy surveys. The baryon acoustic oscillations that occur in the relativistic plasma come in the form of a characteristic peak in the galaxy correlation function. The BAO measurements are usually given in the literature as  $d_V^{th}(z) \equiv r_d/D_V(z)$ , namely the ratio between the comoving sound horizon at the drag epoch ( $r_d$ ) and the spherically averaged distance measure introduced in [39]:

$$D_V(z) = \left[ \frac{d_L^2(z)}{(1+z)^2} \frac{c}{H(z)} \right]^{1/3}. \quad (41)$$

We construct the normalized likelihood function for the BAO data using the six uncorrelated and model-independent measurements given in [38], which we list in Appendix C:

$$\mathcal{L}_{BAO} = \frac{\exp \left[ -\frac{1}{2} \sum_{i=1}^6 \left( \frac{d_V^{th}(z_i) - d_V^{obs}(z_i)}{\sigma_{d_V,i}} \right)^2 \right]}{\left[ (2\pi)^6 \prod_{i=1}^6 \sigma_{d_V,i}^2 \right]^{1/2}}. \quad (42)$$

### D. Results of the Monte Carlo analysis

To test the different cosmographic approaches, we performed a Markov Chain Monte Carlo (MCMC) integration on the combined likelihood of the datasets we presented above:

$$\mathcal{L}_{joint} = \mathcal{L}_{SN} \times \mathcal{L}_{OHD} \times \mathcal{L}_{BAO}. \quad (43)$$

We implemented the Metropolis-Hastings algorithm with the Monte Python code [40], assuming uniform priors for the parameters (see Table I). The numerical results of our

Parameters	Priors
$H_0$	(50, 90)
$q_0$	(-10, 10)
$j_0$	(-10, 10)
$s_0$	(-10, 10)
$M$	(-20, -18)
$\Delta_M$	(-1, 1)
$\alpha$	(0, 1)
$\beta$	(0, 5)
$r_d$	(140, 160)

TABLE I. Priors for parameters estimate in the MCMC numerical analysis.  $H_0$  values are given in units of Km/s/Mpc, while  $r_d$  values in units of Mpc.

joint analysis are shown in Table II. Also, in Figs. 4 to 6 we show the marginalized 2D  $1\sigma$  and  $2\sigma$  regions and the 1D posterior distributions for the cosmological and nuisance parameters in the case of the three cosmographic techniques. Our results prove that the method of rational Chebyshev polynomials reduces the uncertainties in the estimate of the cosmographic parameters with respect to the other approaches, as shown by the relative errors in Table III.

An alternative approach is to start from the cosmographic expansion series of the Hubble rate and, then, evaluate the luminosity distance by numerical integrations, as pointed out in [41]. However, it turns out that the analysis based on rational Chebyshev approximations of  $H(z)$  does not lead to further reduction of the error propagation with respect to our original approach.

Parameter	Taylor			Padé			Rational Chebyshev		
	Mean	$1\sigma$	$2\sigma$	Mean	$1\sigma$	$2\sigma$	Mean	$1\sigma$	$2\sigma$
$H_0$	65.80	+2.09 -2.11	+4.22 -4.00	64.94	+2.11 -2.02	+4.12 -4.13	64.95	+1.89 -1.94	+3.77 -3.77
$q_0$	-0.276	+0.043 -0.049	+0.093 -0.091	-0.285	+0.040 -0.046	+0.087 -0.084	-0.278	+0.021 -0.021	+0.041 -0.042
$j_0$	-0.023	+0.317 -0.397	+0.748 -0.685	0.545	+0.463 -0.652	+1.135 -1.025	1.585	+0.497 -0.914	+1.594 -1.453
$s_0$	-0.745	+0.196 -0.284	+0.564 -0.487	0.118	+0.451 -1.600	+3.422 -1.921	1.041	+1.183 -1.784	+3.388 -3.087
$M$	-19.16	+0.07 -0.07	+0.14 -0.14	-19.03	+0.02 -0.02	+0.05 -0.05	-19.17	+0.07 -0.07	+0.13 -0.13
$\Delta_M$	-0.054	+0.023 -0.022	+0.044 -0.045	-0.054	+0.022 -0.023	+0.045 -0.045	-0.050	+0.022 -0.022	+0.044 -0.045
$\alpha$	0.127	+0.006 -0.006	+0.012 -0.012	0.127	+0.006 -0.006	+0.012 -0.012	0.130	+0.006 -0.006	+0.012 -0.012
$\beta$	2.624	+0.071 -0.068	+0.136 -0.140	2.625	+0.065 -0.069	+0.137 -0.135	2.667	+0.068 -0.069	+0.137 -0.135
$r_d$	149.2	+3.7 -4.1	+7.7 -7.5	148.6	+3.5 -3.8	+7.5 -7.1	147.2	+3.7 -4.0	+7.8 -7.5

TABLE II. 68% and 95% confidence level parameter constraints from the MCMC analysis of SN+OHD+BAO data for the fourth-order Taylor, (2,2) Padé and (2,1) rational Chebyshev polynomial approximations of the luminosity distance.  $H_0$  values are given in units of Km/s/Mpc, while  $r_d$  values in units of Mpc.

Parameter	Taylor		Padé		Rational Chebyshev	
	$1\sigma$	$2\sigma$	$1\sigma$	$2\sigma$	$1\sigma$	$2\sigma$
$H_0$	3.19%	6.25%	3.17%	6.35%	2.95%	4.11%
$q_0$	16.8%	33.5%	15.1%	30.1%	7.66%	14.8%
$j_0$	1534%	3079%	102%	198%	44.5%	96.1%
$s_0$	32.2%	70.5%	866%	2258%	142%	311%

TABLE III. 68% and 95% relative uncertainties on the estimate of the cosmographic parameters from the MCMC analysis of SN+OHD+BAO data for the fourth-order Taylor, (2,2) Padé and (2,1) rational Chebyshev polynomial approximations of the luminosity distance.



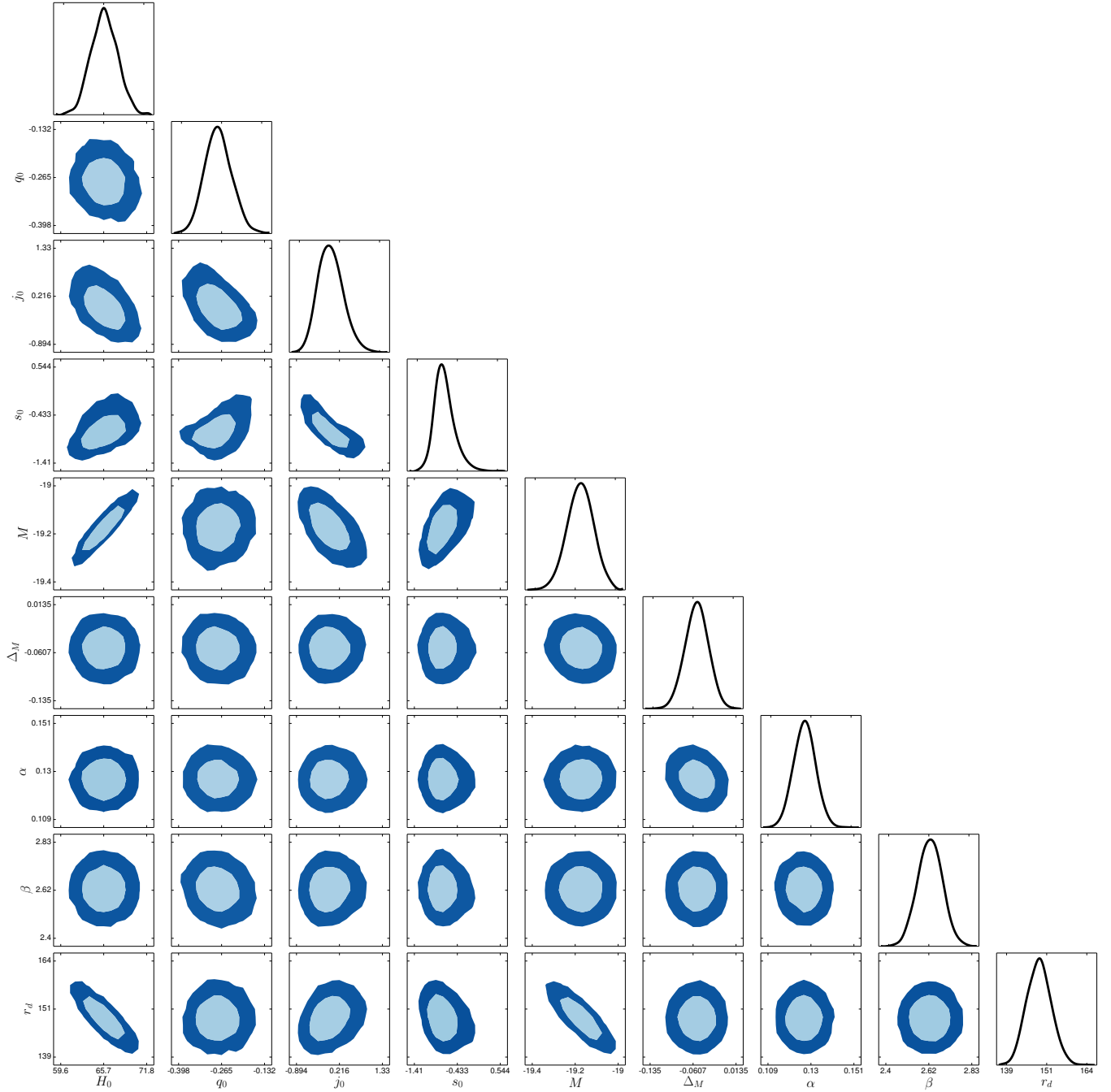


FIG. 4. 68% and 95% confidence level contours and posterior distributions from the MCMC analysis of SN+OHD+BAO data for the fourth-order Taylor approximation of the luminosity distance.  $H_0$  is expressed in Km/s/Mpc, and  $r_d$  in Mpc.

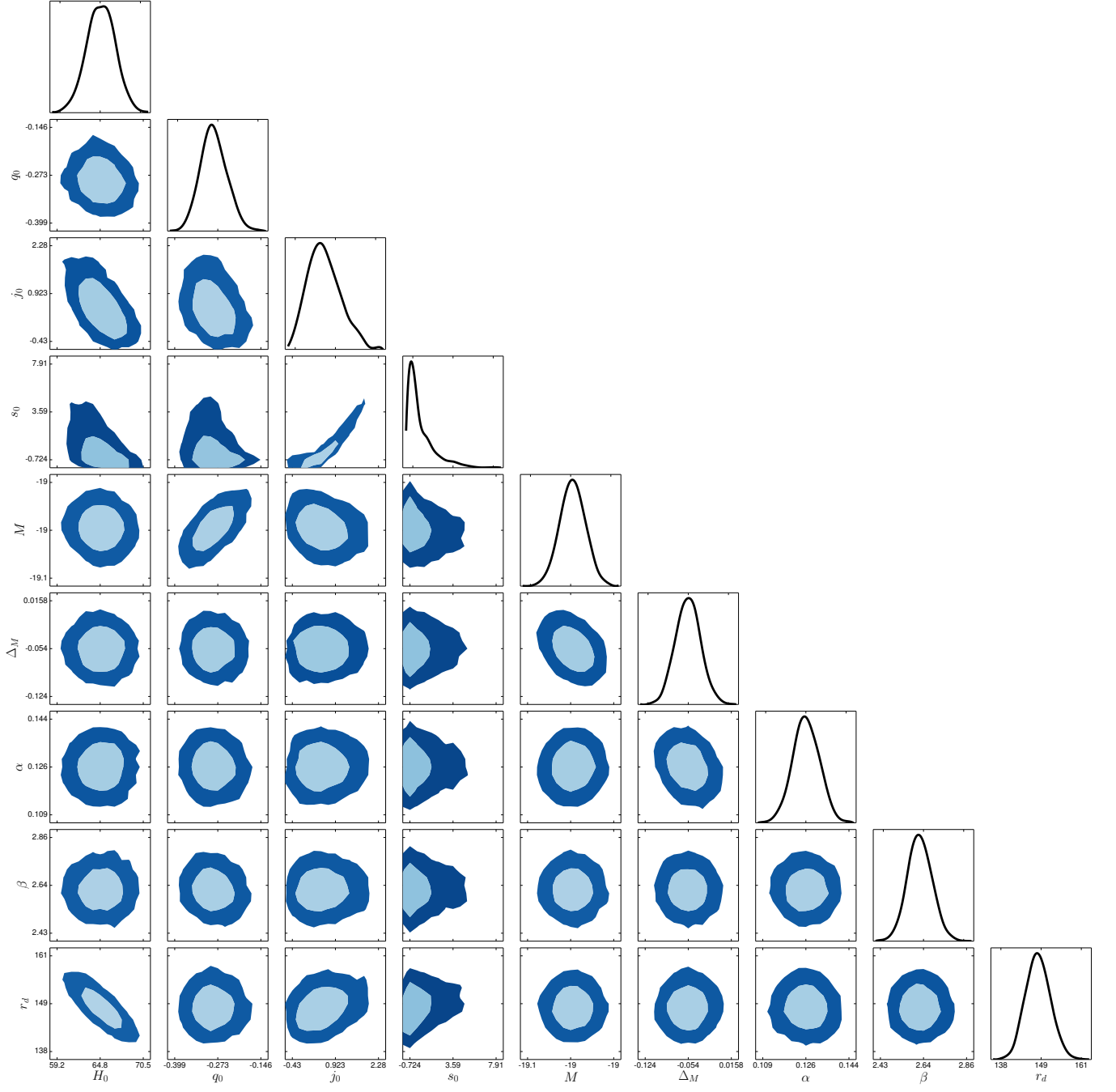


FIG. 5. 68% and 95% confidence level contours and posterior distributions from the MCMC analysis of SN+OHD+BAO data for the (2,2) Padé approximation of the luminosity distance.  $H_0$  is expressed in Km/s/Mpc, and  $r_d$  in Mpc.

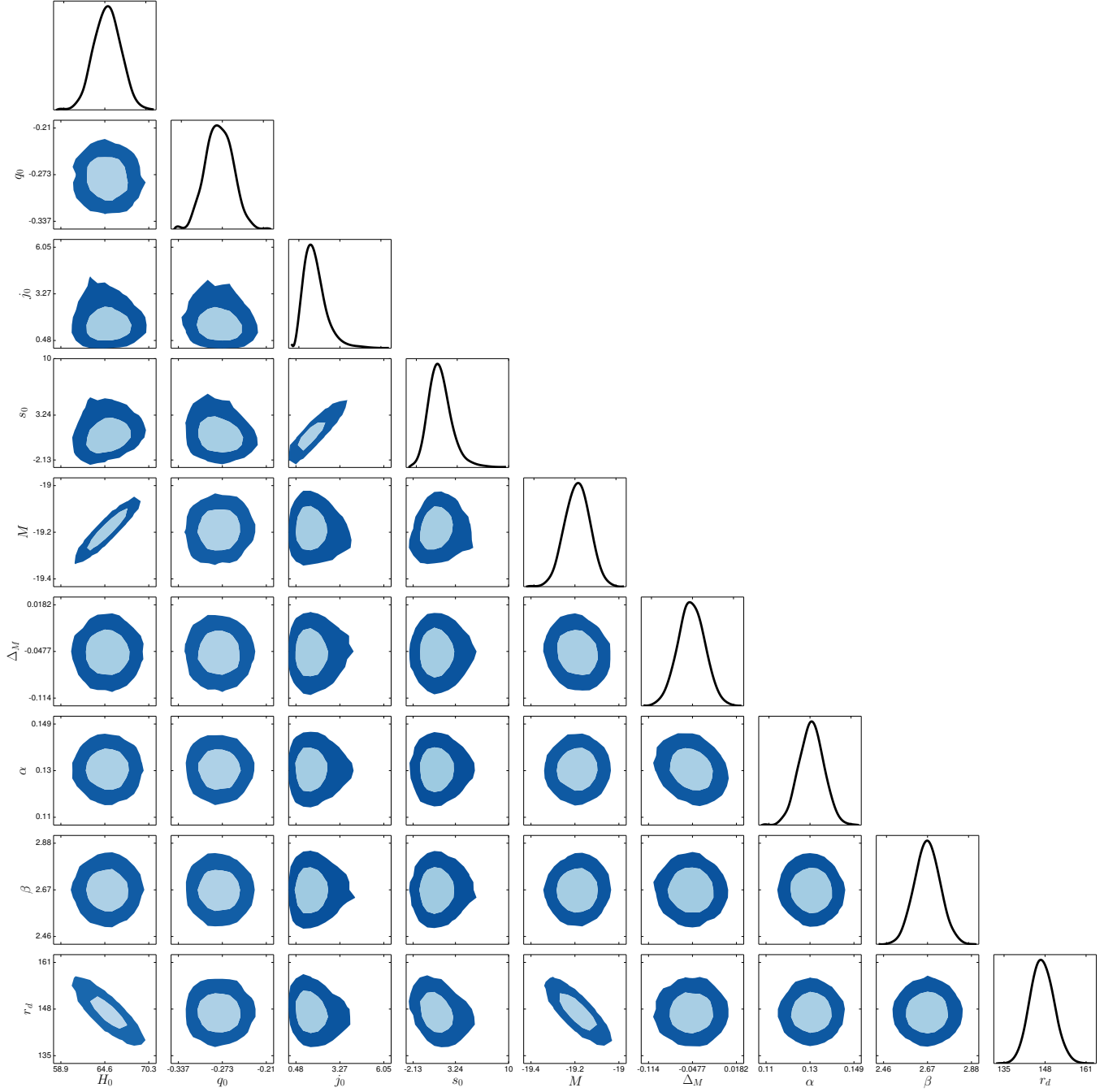


FIG. 6. 68% and 95% confidence level contours and posterior distributions from the MCMC analysis of SN+OHD+BAO data for the (2,1) rational Chebyshev approximation of the luminosity distance.  $H_0$  is expressed in Km/s/Mpc, and  $r_d$  in Mpc.

## VI. SUMMARY AND CONCLUSIONS

In this work, we revised the convergence problem in cosmography, adopting a new method to reduce error uncertainties and bias propagations as high-redshift data are used. We set bounds on the cosmographic series, considering rational approximations of the luminosity distance and we demonstrated that such approximations are also valid for any cosmic distances. In particular, our novel procedure is based on approximating the luminosity distance  $d_L(z)$  with ratios of Chebyshev polynomials. Since, by definition, Chebyshev approximants are the most suitable polynomials in approximating functions, we expected to get fairly good outcomes in computing cosmographic series. Indeed, we found that our approach overcomes the convergence issues typical of standard cosmographic techniques based on Taylor approximations. This has been confirmed by computing convergence radii for different sets of cosmographic coefficients. We also compared our new approach with the consolidate procedure of Padé expansions. We showed that both numerical bounds and convergence radii are improved under precise conditions. This naturally showed that Chebyshev rational polynomials are more suitable to describe the cosmic dynamics at  $z > 1$  than Padé series. Bearing this in mind, through the predictions of the concordance  $\Lambda$ CDM model, we calibrated the orders of Chebyshev rational polynomials, providing the recipe of a new Chebyshev cosmography, which turned out to be more predictive than Taylor series at all redshift domains. We evaluated the (2,1) Chebyshev series, corresponding to a fourth-order Taylor series and to a (2,2) Padé approximation. This showed that lower order Chebyshev series work better than higher ones constructed by Taylor and Padé recipes. We finally checked the goodness of our method, statistically combining the JLA supernova compilation,  $H(z)$  differential age data and baryon acoustic

oscillation measurements by performing Monte Carlo integrations based on the Metropolis-Hastings algorithm. To do so, we employed the free available Monte Python code and we computed the corresponding contours up to the 95% confidence level. The numerical improvements have been reported in terms of percentages on  $1\sigma$  and  $2\sigma$  confidence levels. The error percentages are severely lowered whereas the mean values are centred around intervals compatible with previous results on cosmography.

Our final outcomes forecast that the technique of Chebyshev cosmography substantially decreases the relative uncertainties on the estimates of cosmographic parameters respect to other previous approaches. This procedure candidates as a new way toward computing the cosmographic series and to better fix constraints on cosmography. Chebyshev cosmography is thus able to heal previous inconsistencies on convergence which plagued cosmography itself. Further, it enables to use high-redshift data surveys in cosmographic analyses with no large spreads over fitted coefficients.

Future efforts will be devoted to match Padé and Chebyshev techniques in different redshift domains. We will work on characterizing the cosmographic data over binning intervals in which one will be able to highly maximize both the convergence radii and mean values and to minimize both bias and uncertainties on free cosmographic coefficients.

## ACKNOWLEDGEMENTS

This paper is based upon work from COST action CA15117 (CANTATA), supported by COST (European Cooperation in Science and Technology). S.C. acknowledges the support of INFN (iniziativa specifica QGSKY). R.D. thanks Federico Tosone for useful discussions on the Monte Python code.

- 
- [1] A. G. Riess et al., *Astron. J.*, **116**, 1009-1038, (1998).
  - [2] S. Perlmutter et al., *Astrophys. J.*, **517**, 565-586 (1999).
  - [3] P. A. R. Ade et al. [*Planck Collaboration*], *Astron. Astrophys.*, **594**, A13 (2016).
  - [4] M. Visser, *Classical Quantum Gravity* **21**, 2603 (2004).
  - [5] C. Cattoen, M. Visser, *Classical Quantum Gravity*, **24**, 5985 (2007).
  - [6] T. D. Saini, S. Raychaudhury, V. Sahni, A. A. Starobinsky, *Phys. Rev. Lett.*, **85**, 1162 (2000).
  - [7] R. Cai, Z. Tuo, *Phys. Lett. B*, **706**, 116 (2011).
  - [8] A. C. C. Guimaraes, J. A. S. Lima, *Classical Quantum Gravity*, **28**, 125026 (2011).
  - [9] M. Arabsalmani, V. Sahni, *Phys. Rev. D*, **83**, 04350 (2011).
  - [10] J. C. Carvalho, J. S. Alcaniz, *Mon. Not. Roy. Astron. Soc.*, **418**, 1873-1877 (2011).
  - [11] O. Luongo, *Mod. Phys. Lett. A*, **26**, 1459 (2011).
  - [12] S. Capozziello, R. Lazkoz, V. Salzano, *Phys. Rev. D*, **84**, 124061 (2011).
  - [13] C. Gruber, O. Luongo, *Phys. Rev. D*, **89**, 103506 (2014).
  - [14] H. Wei, X.-P. Yan, and Y.-N. Zhou, *J. Cosmol. Astropart. Phys.*, **01** (2014).
  - [15] S. Weinberg, *Gravitation and Cosmology: Principles and Applications of the General Theory of Relativity*, Wiley, Hoboken, NJ, USA, (1972).
  - [16] M. Visser, *Science*, **276**, 88 (1997).
  - [17] E. R. Harrison, *Nature*, **260**, 591 (1976).
  - [18] P. K. S. Dunsby, O. Luongo, *Int. J. Geom. Meth. Mod. Phys.*, **13**, 1630002 (2016).
  - [19] M. Visser, *Gen. Rel. Grav.*, **37**, 1541-1548 (2005).
  - [20] M. Visser, *Class. Quant. Grav.*, **32**, 135007 (2015).
  - [21] N. Poplawski, *Phys. Lett. B*, **640**, 135 (2006).
  - [22] N. Poplawski, *Class. Quant. Grav.*, **24**, 3013 (2007).
  - [23] C. Cattoen, M. Visser, *Phys. Rev. D*, **78**, 063501 (2008).
  - [24] L. Xu, Y. Wang, *Phys. Lett. B*, **702**, 114-120 (2011).
  - [25] A. Aviles, C. Gruber, O. Luongo, H. Quevedo, *Phys. Rev. D*, **86**, 123516 (2012).
  - [26] V. C. Busti et al., *Phys. Rev. D*, **92**, 123512 (2015).

- [27] M. Demianski et al., *Mon. Not. Roy. Astron. Soc.*, **426**, 1396 (2012).
- [28] E. Piedipalumbo et al., *Intern. Jour. Mod. Phys. D*, **24**, 1550100 (2015).
- [29] M. Demianski et al., *Astron. Astroph.*, **598**, A113 (2017).
- [30] G. A. Baker Jr., P. Graves-Morris, *Padé Approximants*, Cambridge University Press (1996).
- [31] G. Litvinov, *Appl. Russ. J. Math. Phys.*, **1**(3), 313-352 (1993).
- [32] P. L. Chebyshev, *Mémoires des Savants étrangers présentés à l'Académie de Saint-Pétersbourg*, **7**, 539-586 (1854).
- [33] C. F. Gerald, P. O. Wheatley, *Applied Numerical Analysis*, Prentice Hall College Div (2003).
- [34] A. Aviles, A. Bravetti, S. Capozziello, O. Luongo, *Phys. Rev. D*, **90**, 043531 (2014).
- [35] M. Betoule et al., *Astron. Astrophys.*, **568**, A22 (2014).
- [36] J. Guy et al., *Astron. Astrophys.*, **466**, 11 (2007).
- [37] R. Jimenez, A. Loeb, *Astrophys. J.*, **573**, 37 (2002).
- [38] V. Lukovic, R. D'Agostino, N. Vittorio, *Astron. Astrophys.*, **595**, A109 (2016).
- [39] D. J. Eisenstein et al., *Astrophys. J.*, **633**, 560-574 (2005).
- [40] B. Audren, J. Lesgourgues, K. Benabed, S. Prunet, *JCAP*, **02**, 001 (2013).
- [41] A. Aviles, J. Klapp, O. Luongo, *Phys. Dark Univ.* **17**, 25-37 (2017).
- [42] C. Zhang et al., *Res. Astron. Astrophys.*, **14**, 1221 (2014).
- [43] J. Simon, L. Verde, R. Jimenez, *Phys. Rev. D*, **71**, 123001 (2005).
- [44] M. Moresco et al., *J. Cosmol. Astropart. Phys.*, **8**, 006 (2012).
- [45] C.-H. Chuang et al., *Mon. Not. R. Astron. Soc.*, **426**, 226 (2012).
- [46] M. Moresco et al., *J. Cosmol. Astropart. Phys.*, **05**, 014 (2016).
- [47] D. Stern, R. Jimenez, L. Verde, S. A. Stanford, M. Kamionkowski, *ApJS*, **188**, 280 (2010).
- [48] M. Moresco, *Mon. Not. R. Astron. Soc.*, **450**, L16 (2015).
- [49] F. Beutler et al., *Mon. Not. R. Astron. Soc.*, **416**, 3017 (2011).
- [50] A. Ross et al., *Mon. Not. R. Astron. Soc.*, **449**, 835 (2015).
- [51] L. Anderson et al., *Mon. Not. R. Astron. Soc.*, **441**, 24 (2014).
- [52] T. Delubac et al., *Astron. Astrophys.*, **574**, A59 (2015).
- [53] A. Font-Ribera et al., *J. Cosmology Astropart. Phys.*, **5**, 27 (2014).

**Appendix A: Rational Chebyshev approximations of the luminosity distance**

In this appendix, we write the rational Chebyshev approximations of the luminosity distance up to the fourth degree:

$$\begin{aligned}
 R_{1,1}(z) = & -\frac{c}{H_0} \left[ (3(2 - 2q_0 - 15q_0^2 - 15q_0^3 + 5j_0(1 + 2q_0) + s_0) + (1/(7 - j_0 + q_0 + 3q_0^2))(-72(7 - j_0 + q_0 + 3q_0^2)^2 \right. \\
 & + 3(18 + 5j_0(1 + 2q_0) - 3q_0(6 + 5q_0(1 + q_0)) + s_0)(14 + 5j_0(1 + 2q_0) - q_0(14 + 15q_0(1 + q_0)) + s_0) \\
 & + 2(14 + 5j_0(1 + 2q_0) - q_0(14 + 15q_0(1 + q_0)) + s_0)^2)z \Big/ (576(1 - ((14 + 5j_0(1 + 2q_0) - q_0(14 + 15q_0(1 + q_0)) \\
 & + s_0)z)/(3(7 - j_0 + q_0 + 3q_0^2)))) \Big] , \tag{A1}
 \end{aligned}$$

$$\begin{aligned}
 R_{1,2}(z) = & \frac{c}{H_0} ( -((44184 + 5j_0^3(1 + 2q_0)(1 + 10q_0)(9 + 10q_0) - 3q_0(32024 + q_0(26948 + q_0(4780 + q_0(-15938 + q_0(2134 \\
 & + 15q_0(565 + 3q_0(249 + 25q_0(3 + q_0)))))) + 7148s_0 + q_0(-5272 + q_0(-16 + 3q_0(-32 + 3q_0(439 + 75q_0(2 \\
 & + q_0))))s_0 - 3(-38 + q_0(38 + 15q_0(1 + q_0)))s_0^2 + s_0^3 + j_0(49884 + q_0(34880 + q_0(-41632 + q_0(-9472 \\
 & + 135q_0(125 + q_0(332 + 25q_0(5 + 2q_0)))))) + 916s_0 - 2q_0(-586 + 3q_0(439 + 75q_0(3 + 2q_0)))s_0 + 15(1 + 2q_0)s_0^2) \\
 & + j_0^2(-222 + 59s_0 + q_0(8422 - 5q_0(17 + 15q_0(211 + 60q_0(2 + q_0)) - 60s_0) + 300s_0)))/(8(-1 - j_0 + q_0 + 3q_0^2)(7 \\
 & - j_0 + q_0 + 3q_0^2) + 24(7 - j_0 + q_0 + 3q_0^2)^2 - (18 + 5j_0(1 + 2q_0) - 3q_0(6 + 5q_0(1 + q_0)) + s_0)(14 + 5j_0(1 + 2q_0) \\
 & - q_0(14 + 15q_0(1 + q_0))s_0)) + 4(271 - 17j_0 + 17q_0 + 51q_0^2 + (4(39106 - 56j_0^3 + j_0^2(1665 + q_0(193 + 454q_0)) \\
 & + 5s_0 - j_0(14469 - 5s_0 + q_0(3492 + q_0(10127 + q_0(1033 + 1287q_0)) + 5s_0)) + q_0(14282 - 10s_0 + q_0(45365 \\
 & - 10s_0 + q_0(10501 + 3q_0(5082 + q_0(479 + 429q_0)) + 15s_0)))))/(-868 + j_0^2(-7 + 100q_0(1 + q_0)) + q_0(-888 \\
 & + q_0(-1412 + 3q_0(-64 + q_0(139 + 75q_0(2 + q_0)))))) + 32s_0 - 2q_0(16 + 15q_0(1 + q_0))s_0 + s_0^2 + j_0(544 + 10s_0 \\
 & - 2q_0(q_0(139 + 75q_0(3 + 2q_0)) - 2(56 + 5s_0))))z \Big/ (576(1 - (4(214 - 5j_0^2(1 + 2q_0) + j_0(65 + 5q_0(33 + q_0(8 \\
 & + 9q_0)) - s_0) + 15s_0 + q_0(-204 - 5q_0(41 + 3q_0(18 + q_0(4 + 3q_0))) + s_0 + 3q_0s_0))z)/(8(-1 - j_0 + q_0 + 3q_0^2)(7 \\
 & - j_0 + q_0 + 3q_0^2) + 24(7 - j_0 + q_0 + 3q_0^2)^2 - (18 + 5j_0(1 + 2q_0) - 3q_0(6 + 5q_0(1 + q_0)) + s_0)(14 + 5j_0(1 + 2q_0) \\
 & - q_0(14 + 15q_0(1 + q_0)) + s_0)) - (4(12(-1 - j_0 + q_0 + 3q_0^2)(7 - j_0 + q_0 + 3q_0^2) + 4(1 + j_0 - q_0(1 + 3q_0)))^2 \\
 & - (14 + 5j_0(1 + 2q_0) - q_0(14 + 15q_0(1 + q_0)) + s_0)^2)(-1 + 2z^2))/(3(8(-1 - j_0 + q_0 + 3q_0^2)(7 - j_0 + q_0 + 3q_0^2) \\
 & + 24(7 - j_0 + q_0 + 3q_0^2)^2 - (18 + 5j_0(1 + 2q_0) - 3q_0(6 + 5q_0(1 + q_0)) + s_0)(14 + 5j_0(1 + 2q_0) - q_0(14 \\
 & + 15q_0(1 + q_0)) + s_0)))) , \tag{A2}
 \end{aligned}$$

$$\begin{aligned}
 R_{2,1}(z) = & \frac{c}{H_0} ( -((3(16(-1 - j_0 + q_0 + 3q_0^2)(7 - j_0 + q_0 + 3q_0^2) - (18 + 5j_0(1 + 2q_0) - 3q_0(6 + 5q_0(1 + q_0)) + s_0)(14 \\
 & + 5j_0(1 + 2q_0) - q_0(14 + 15q_0(1 + q_0)) + s_0)))/(14 + 5j_0(1 + 2q_0) - q_0(14 + 15q_0(1 + q_0)) + s_0) + 4(47 - j_0 \\
 & + q_0 + 3q_0^2 - (12(-1 + q_0)(1 + j_0 - q_0(1 + 3q_0)))/(14 + 5j_0(1 + 2q_0) - q_0(14 + 15q_0(1 + q_0)) + s_0))z \\
 & - (4(12(-1 - j_0 + q_0 + 3q_0^2)(7 - j_0 + q_0 + 3q_0^2) + 4(1 + j_0 - q_0(1 + 3q_0)))^2 - (14 + 5j_0(1 + 2q_0) - q_0(14 \\
 & + 15q_0(1 + q_0)) + s_0)^2)(-1 + 2z^2))/(14 + 5j_0(1 + 2q_0) - q_0(14 + 15q_0(1 + q_0)) + s_0) \Big/ (192(1 + (4(1 + j_0 \\
 & - q_0(1 + 3q_0))z)/(14 + 5j_0(1 + 2q_0) - q_0(14 + 15q_0(1 + q_0)) + s_0)) , \tag{A3}
 \end{aligned}$$

$$\begin{aligned}
R_{1,3}(z) = & -\frac{c}{H_0} \left[ (1561600 + 534784s_0 + 41472s_0^2 + 1344s_0^3 + 143726992z + 48790350q_0^{10}z + 21262500q_0^{11}z + 5315625q_0^{12}z \right. \\
& + 15j_0^4(-489 - 840q_0 + 69160q_0^2 + 140000q_0^3 + 70000q_0^4)z - 14619744s_0z - 300520s_0^2z + 8232s_0^3z + 105s_0^4z \\
& - 56700q_0^9(48 + (-843 + 25s_0)z) - 675q_0^8(16576 + (92213 + 6300s_0)z) - 180q_0^7(106896 + 7(195524 + 6633s_0)z) \\
& - 8q_0(584896 + s_0(118144 - 620452z)) - 44133176z + 1029s_0^3z + s_0^2(5520 + 72838z)) + 12q_0^5(677344 - 25916176z \\
& + 23625s_0^2z + 6s_0(24080 + 153453z)) - 4q_0^2(1575s_0^3z + 12s_0^2(1372 + 9637z)) - 4s_0(-90320 + 653249z) \\
& - 192(-9337 + 762081z)) + 2q_0^4(231903s_0^2z + 36s_0(27672 + 350209z) + 4(3013792 + 3194005z)) - 4q_0^3(1575s_0^3z \\
& + 1008s_0^2(13 + 8z) - 20s_0(3984 + 419287z) - 32(93610 + 3209821z)) + 6q_0^6(23625s_0^2z - 630s_0(-176 + 1205z) \\
& - 4(576840 + 17866679z)) - 20j_0^3(-4592 + 878430q_0^4z + 787500q_0^5z + 315000q_0^6z + (-27002 + 63s_0)z \\
& - 105q_0^3(512 + 5(-277 + 40s_0)z) - 2q_0(26144 + (374833 + 5187s_0)z) - q_0^2(100800 + (1004813 + 31500s_0)z)) \\
& + 2j_0^2(33693975q_0^6z + 21262500q_0^7z + 7087500q_0^8z + 5187s_0^2z + 348(3456 + 52589z) + s_0(53600 + 751068z) \\
& - 3150q_0^5(704 + 25(-191 + 12s_0)z) - 30q_0^3(187152 + (2523232 + 67095s_0)z) - 15q_0^4(380800 + (3084503 \\
& + 126000s_0)z) + 4q_0(587248 - 1747434z + 7875s_0^2z + s_0(53760 + 539493z)) + 2q_0^2(15750s_0^2z + 105s_0(832 \\
& + 539z) - 4(114020 + 7726509z))) - 4j_0(24395175q_0^8z + 12403125q_0^9z + 3543750q_0^{10}z - 525s_0^3z - 2s_0^2(2856 \\
& + 28939z) - 4s_0(40160 + 41679z) + 24(-42472 + 1941285z) - 23625q_0^7(64 + 5(-149 + 6s_0)z) - 225q_0^6(22288 \\
& + (150091 + 7875s_0)z) - 30q_0^5(228144 + (2980493 + 92862s_0)z) + q_0^3(3597632 - 51966500z + 70875s_0^2z \\
& + 48s_0(9590 + 74537z)) + q_0^2(4962368 + 22362652z + 77301s_0^2z + 8s_0(44604 + 585577z)) - 2q_0(525s_0^3z \\
& + 21s_0^2(224 + 799z) - 32s_0(-1111 + 59056z) - 4(65536 + 7419921z)) + q_0^4(47250s_0^2z - 945s_0(-256 + 715z) \\
& - 2(1501320 + 59053033z)))/ (384(-247152 + 68112s_0 + 2340s_0^2 + 50376z - 59124s_0z - 3114s_0^2z - 63s_0^3z \\
& - 556608z^2 - 66624s_0z^2 - 2448s_0^2z^2 + 502496z^3 + 94928s_0z^3 + 2856s_0^2z^3 + 60s_0^3z^3 - 10125q_0^9z(-21 + 20z^2) \\
& - 2025q_0^8(-84 - 315z + 80z^2 + 300z^3) - 135q_0^7(-2940 - 8955z + 2800z^2 + 8492z^3) + 27q_0^6(37440 - 25(-1033 \\
& + 63s_0)z - 36608z^2 + 300(-83 + 5s_0)z^3) + q_0^3(-716352 - 1083156z + 438528z^2 + 53072z^3 - 135s_0^2z(-21 + 20z^2) \\
& - 144s_0(681 - 40z - 676z^2 + 32z^3)) + 18q_0^5(61530 - 32087z - 64232z^2 + 15388z^3 + 15s_0(-84 - 315z + 80z^2 \\
& + 300z^3)) + 3j_0^3(-820 - 1025z + 976z^2 + 1220z^3 + 1000q_0^3z(-21 + 20z^2) + 100q_0^2(-84 - 315z + 80z^2 + 300z^3) \\
& + 10q_0(-840 - 1255z + 800z^2 + 1244z^3)) + q_0^2(-1759344 + 571812z + 933312z^2 - 1082768z^3 - 9s_0^2(-84 - 315z \\
& + 80z^2 + 300z^3) - 24s_0(2361 - 2725z - 2596z^2 + 1812z^3)) - 2q_0(643992 - 369876z - 448608z^2 + 555088z^3 \\
& + 3s_0^2(-42 - 519z + 40z^2 + 476z^3) + 4s_0(7668 - 13629z - 7632z^2 + 11188z^3)) + 3q_0^4(238140 - 615186z \\
& - 326640z^2 + 428744z^3 + 3s_0(-3360 - 14145z + 3200z^2 + 13252z^3)) + j_0^2(-43692 - 90906z + 6576z^2 + 51944z^3 \\
& - 13500q_0^5z(-21 + 20z^2) - 1800q_0^4(-84 - 315z + 80z^2 + 300z^3) + 3s_0(-840 - 1255z + 800z^2 + 1244z^3) \\
& - 75q_0^3(-2856 - 7917z + 2720z^2 + 7540z^3) + 3q_0^2(116340 + (2825 - 6300s_0)z - 116944z^2 + 20(-293 + 300s_0)z^3) \\
& + 2q_0(97470 - 169767z - 106872z^2 + 124508z^3 + 30s_0(-84 - 315z + 80z^2 + 300z^3))) + j_0(692832 - 537540z \\
& - 418176z^2 + 631312z^3 + 20250q_0^7z(-21 + 20z^2) + 3375q_0^6(-84 - 315z + 80z^2 + 300z^3) + 3s_0^2(-84 - 315z \\
& + 80z^2 + 300z^3) + 4s_0(4158 - 9609z - 4728z^2 + 7268z^3) + 180q_0^5(-2940 - 8955z + 2800z^2 + 8492z^3) \\
& - 9q_0^4(131820 - 225(-229 + 28s_0)z - 130224z^2 + 100(-509 + 60s_0)z^3) + 2q_0(45s_0^2z(-21 + 20z^2) + 6s_0(4674 \\
& - 2755z - 4744z^2 + 2508z^3) + 16(18483 + 4656z - 15180z^2 + 12160z^3)) - 6q_0^3(45s_0(-84 - 315z + 80z^2 + 300z^3) \\
& + 8(20580 - 20033z - 21968z^2 + 12932z^3)) - 6q_0^2(s_0(-3360 - 14145z + 3200z^2 + 13252z^3) + 4(17241 - 59711z \\
& - 25508z^2 + 43004z^3)))] , \tag{A4}
\end{aligned}$$

$$\begin{aligned}
R_{2,2}(z) = & -\frac{c}{H_0} \left[ (2808 + 3828s_0 + 474s_0^2 + 15s_0^3 + 891712z + 115776s_0z + 4560s_0^2z + 753744z^2 + 142392s_0z^2 + 4284s_0^2z^2 \right. \\
& + 90s_0^3z^2 - 50625q_0^9(1 + 6z^2) - 10125q_0^8(15 - 16z + 90z^2) - 135q_0^7(1723 - 2800z + 12738z^2) + 135q_0^6(-845 \\
& + 10688z - 7470z^2 + 75s_0(1 + 6z^2)) - q_0^3(-13140 + 440320z - 79608z^2 + 675s_0^2(1 + 6z^2) + 576s_0(2 + 275z \\
& + 12z^2)) + 18q_0^5(4463 + 117160z + 23082z^2 + 75s_0(15 - 16z + 90z^2)) + 5j_0^3(183 - 688z + 1098z^2 + 3000q_0^3(1 \\
& + 6z^2) + 300q_0^2(15 - 16z + 90z^2) + 6q_0(311 - 800z + 1866z^2)) - 3q_0^2(9420 + 555072z + 541384z^2 + 15s_0^2(15 - \\
& 16z + 90z^2) + 8s_0(385 + 5300z + 2718z^2)) + 9q_0^4(15158 + 229520z + 214372z^2 + s_0(2513 - 3200z + 19878z^2)) \\
& - 6q_0(s_0^2(79 - 40z + 714z^2) + 4s_0(319 + 4624z + 5594z^2) + 4(351 + 61768z + 69386z^2)) - 3j_0^2(s_0(-311 + 800z \\
& - 1866z^2) + 22500q_0^5(1 + 6z^2) + 3000q_0^4(15 - 16z + 90z^2) + 125q_0^3(313 - 544z + 2262z^2) - 2(1079 + 6040z \\
& + 12986z^2) - 5q_0^2(-293 + 37264z - 1758z^2 + 300s_0(1 + 6z^2)) - 2q_0(6181 + 71720z + 62254z^2 + 50s_0(15 - 16z \\
& + 90z^2))) + 3j_0(33750q_0^7(1 + 6z^2) + 5625q_0^6(15 - 16z + 90z^2) + 5s_0^2(15 - 16z + 90z^2) + 4s_0(363 + 3400z \\
& + 3634z^2) + 60q_0^5(1723 - 2800z + 12738z^2) + 4(1019 + 62496z + 78914z^2) - 15q_0^4(-1745 + 39664z - 15270z^2 \\
& + 300s_0(1 + 6z^2)) + 2q_0(75s_0^2(1 + 6z^2) + 64(36 + 1895z + 1520z^2) + 2s_0(427 + 8200z + 3762z^2)) - 2q_0^3(225s_0(15 \\
& - 16z + 90z^2) + 8(2477 + 42040z + 19398z^2)) - 2q_0^2(s_0(2513 - 3200z + 19878z^2) + 12(1433 + 18780z \\
& + 21502z^2)))) / (384(-2348 - 324s_0 - 15s_0^2 - 784z - 200s_0z + 104z^2 + 136s_0z^2 + 10s_0^2z^2 + 1125q_0^6(-3 + 2z^2) \\
& + 90q_0^5(-75 - 4z + 50z^2) + q_0^4(-6795 - 480z + 3138z^2) - 6q_0^3(25s_0(-3 + 2z^2) + 8(-20 - 35z + 16z^2)) \\
& - 4q_0(-982 - 296z + 52z^2 + s_0(-81 - 2z + 34z^2)) + j_0^2(-215 - 40z + 122z^2 + 500q_0^2(-3 + 2z^2) + 20q_0(-75 \\
& - 4z + 50z^2)) + q_0^2(8(578 + 475z - 146z^2) - 6s_0(-75 - 4z + 50z^2)) - 2j_0(1034 + 700z - 212z^2 + s_0(75 + 4z \\
& - 50z^2) + 750q_0^4(-3 + 2z^2) + 45q_0^3(-75 - 4z + 50z^2) + q_0^2(-2265 - 160z + 1046z^2) + q_0(970 + 780z - 468z^2 \\
& - 50s_0(-3 + 2z^2))))], \tag{A5}
\end{aligned}$$

$$\begin{aligned}
R_{3,1}(z) = & \frac{c}{H_0} (-(24(-((-1 - j_0 + q_0(1 + 3q_0))(18 + 5j_0(1 + 2q_0) - 3q_0(6 + 5q_0(1 + q_0)) + s_0))/1536) + ((7 - j_0 + q_0 \\
& + 3q_0^2)(2 + 5j_0(1 + 2q_0) - q_0(2 + 15q_0(1 + q_0)) + s_0))/1536)/(-1 - j_0 + q_0(1 + 3q_0))) - (1/(-1 - j_0 + q_0(1 \\
& + 3q_0)))24(-1/192)(7 - j_0 + q_0 + 3q_0^2)(-1 - j_0 + q_0(1 + 3q_0)) + ((18 + 5j_0(1 + 2q_0) - 3q_0(6 + 5q_0(1 + q_0)) \\
& + s_0)(2 + 5j_0(1 + 2q_0) - q_0(2 + 15q_0(1 + q_0)) + s_0))/6144 + (((2 + 5j_0(1 + 2q_0) - q_0(2 + 15q_0(1 + q_0)) + s_0)(14 \\
& + 5j_0(1 + 2q_0) - q_0(14 + 15q_0(1 + q_0)) + s_0))/9216)z - (1/(-1 - j_0 + q_0(1 + 3q_0)))24(((7 - j_0 + q_0 + 3q_0^2)(2 \\
& + 5j_0(1 + 2q_0) - q_0(2 + 15q_0(1 + q_0)) + s_0))/1536 + (((-1 - j_0 + q_0(1 + 3q_0))(2 + 5j_0(1 + 2q_0) - q_0(2 + 15q_0(1 \\
& + q_0)) + s_0))/4608) - (((-1 - j_0 + q_0(1 + 3q_0))(14 + 5j_0(1 + 2q_0) - q_0(14 + 15q_0(1 + q_0)) + s_0))/1152)(-1 + 2z^2) \\
& - 1/(-1 - j_0 + q_0(1 + 3q_0))24(-1/576)(-1 - j_0 + q_0(1 + 3q_0))^2 + (2 + 5j_0(1 + 2q_0) - q_0(2 + 15q_0(1 + q_0)) \\
& + s_0)^2/36864 + (((2 + 5j_0(1 + 2q_0) - q_0(2 + 15q_0(1 + q_0)) + s_0)(14 + 5j_0(1 + 2q_0) - q_0(14 + 15q_0(1 + q_0)) \\
& + s_0))/9216))(-3z + 4z^3)) / (1 - ((2 + 5j_0(1 + 2q_0) - q_0(2 + 15q_0(1 + q_0)) + s_0)z)/(4(-1 - j_0 + q_0(1 + 3q_0))))). \tag{A6}
\end{aligned}$$

### Appendix B: (2,2) Padé approximant of the luminosity distance

We report here the (2,2) Padé approximation of the luminosity distance:

$$\begin{aligned}
P_{2,2}(z) = & \frac{c}{H_0} (6z(10 + 9z - 6q_0^3z + s_0z - 2q_0^2(3 + 7z) - q_0(16 + 19z) + j_0(4 + (9 + 6q_0)z)) / (60 + 24z + 6s_0z - 2z^2 \\
& + 4j_0^2z^2 - 9q_0^4z^2 - 3s_0z^2 + 6q_0^3z(-9 + 4z) + q_0^2(-36 - 114z + 19z^2)). \tag{B1}
\end{aligned}$$



### Appendix C: Experimental data

Here, we list the compilations of OHD data and BAO data used to perform the Monte Carlo analysis.

$z$	$H \pm \sigma_H$	Ref.
0.0708	$69.00 \pm 19.68$	[42]
0.09	$69.0 \pm 12.0$	[37]
0.12	$68.6 \pm 26.2$	[42]
0.17	$83.0 \pm 8.0$	[43]
0.179	$75.0 \pm 4.0$	[44]
0.199	$75.0 \pm 5.0$	[44]
0.20	$72.9 \pm 29.6$	[42]
0.27	$77.0 \pm 14.0$	[43]
0.28	$88.8 \pm 36.6$	[42]
0.35	$82.1 \pm 4.85$	[45]
0.352	$83.0 \pm 14.0$	[46]
0.3802	$83.0 \pm 13.5$	[46]
0.4	$95.0 \pm 17.0$	[43]
0.4004	$77.0 \pm 10.2$	[46]
0.4247	$87.1 \pm 11.2$	[46]
0.4497	$92.8 \pm 12.9$	[46]
0.4783	$80.9 \pm 9.0$	[46]
0.48	$97.0 \pm 62.0$	[47]
0.593	$104.0 \pm 13.0$	[44]
0.68	$92.0 \pm 8.0$	[44]
0.781	$105.0 \pm 12.0$	[44]
0.875	$125.0 \pm 17.0$	[44]
0.88	$90.0 \pm 40.0$	[47]
0.9	$117.0 \pm 23.0$	[43]
1.037	$154.0 \pm 20.0$	[44]
1.3	$168.0 \pm 17.0$	[43]
1.363	$160.0 \pm 33.6$	[48]
1.43	$177.0 \pm 18.0$	[43]
1.53	$140.0 \pm 14.0$	[43]
1.75	$202.0 \pm 40.0$	[43]
1.965	$186.5 \pm 50.4$	[48]

TABLE IV. Differential age  $H(z)$  data used in this work. The Hubble rate is given in units of km/s/Mpc.

$z$	$d_V \pm \sigma_{d_V}$	Survey	Ref.
0.106	$0.336 \pm 0.015$	6dFGS	[49]
0.15	$0.2239 \pm 0.0084$	SDSS DR7	[50]
0.32	$0.1181 \pm 0.0023$	BOSS DR11	[51]
0.57	$0.0726 \pm 0.0007$	BOSS DR11	[51]
2.34	$0.0320 \pm 0.0016$	BOSS DR11	[52]
2.36	$0.0329 \pm 0.0012$	BOSS DR11	[53]

TABLE V. BAO data used in this work.